



Tunable Engineered Extracellular Matrix Materials: Polyelectrolyte Multilayers Promote Improved Neural Cell Growth and Survival

Michael J. Landry, Kaien Gu, Stephanie N. Harris, Laila Al-Alwan, Laura Gutsin, Daniele De Biasio, Bernie Jiang, Diane S. Nakamura, T. Christopher Corkery, Timothy E. Kennedy,* and Christopher J. Barrett*

Poly-D-lysine (PDL) and poly-L-lysine are standard surfaces for culturing neural cells; however, both are relatively unstable, costly, and the coated surface typically must be prepared immediately before use. Here, polyelectrolyte multilayers (PEMs) are employed as highly stable, relatively inexpensive, alternative substrates to support primary neural cell culture. Initial findings identify specific silk-based PEMs that significantly outperform the capacity of PDL to promote neuronal survival and process extension. Based on these results, a library of PEM variants, including commercial and bio-sourced polyelectrolytes, is generated and three silk-based PEMs that substantially outperform PDL as a substrate for primary neurons in cell culture are identified. Further, testing these PEM variants as substrates for primary oligodendrocyte progenitors demonstrates that one silk-based PEM functions significantly better than PDL. These findings reveal specificity of cellular responses, indicating that PEMs may be tuned to optimally support different neural cell types.

mechanical support. The physical properties of a cellular support material are critical, as cells and tissues are sensitive to the modulus of the surface on which they are cultivated.^[1] Therefore, controlling the surface properties of a cell culture substrate, such as surface energy and Young's modulus, impacts cell survival and development. Some cells are more difficult to maintain and grow in cell culture than others, with mammalian primary neural cells being particularly challenging. These include neurons and oligodendrocytes, which are neural cell types directly associated with neurodegenerative disorders such as Alzheimer's and Parkinson's diseases and multiple sclerosis.^[2] The study of neurodegenerative disorders will be facilitated by an in vitro environment that closely mimics the in vivo conditions found within tissue, to provide an optimal

1. Introduction

Precise conditions of temperature, humidity, and nutrition are essential for successful cell culture, along with adequate

platform for testing potential therapeutics. Currently, only a small set of substrate surfaces are typically employed to culture primary neural cells.

A typical "state-of-the-art" culture substrate for primary neural cells is produced by first cleaning a glass surface, and then applying a single layer of poly-D-lysine (PDL) prior to plating the cells. These layers are not robust, can be damaged by drying or UV light, are ultimately degraded by proteolysis, and are not stable in long-term storage. They must, therefore, be prepared immediately prior to plating the cells onto the surface. Poly-L-lysine (PLL) and its "mirror twin" PDL are widely used as standard surfaces to culture neural cells.^[3,4] These polypeptide substrates are thought to function as non-specific attachment factors for cells, driven by electrostatic attraction between the positively charged lysine groups and the electron-negative phospholipid bilayer of the plasma membrane.^[5,6]

There is an opportunity to create improved substrates to 1) better support the growth of neural cells, 2) improve experimental reproducibility, and 3) facilitate neural cell cultivation. An ideal system would use inexpensive, degradation-resistant substrates that are easy to process. Peptides present one class of options, yet protein-decorated surfaces are expensive to produce and suffer from the same degradation limitations as poly-lysine.

Dr. M. J. Landry, K. Gu, S. N. Harris, Dr. L. Al-Alwan, L. Gutsin, D. De Biasio, B. Jiang, D. S. Nakamura, Dr. T. C. Corkery, Prof. T. E. Kennedy, Prof. C. J. Barrett
McGill Program in Neuroengineering
McGill University

3801 University Street, Montreal, QC H3A 2B4, Canada
E-mail: timothy.kennedy@mcgill.ca; christopher.barrett@mcgill.ca

Dr. M. J. Landry, K. Gu, L. Gutsin, D. De Biasio, B. Jiang, Prof. C. J. Barrett
Department of Chemistry
McGill University

801 Sherbrooke St. West, Montreal, QC H3A 0B8, Canada

S. N. Harris, Dr. L. Al-Alwan, D. S. Nakamura, Prof. T. E. Kennedy
Department of Neurology and Neurosurgery
Montreal Neurological Institute
McGill University

3801 University Street, Montreal, QC H3A 2B4, Canada

 The ORCID identification number(s) for the author(s) of this article can be found under <https://doi.org/10.1002/mabi.201900036>.

DOI: 10.1002/mabi.201900036

Previous studies have revealed that materials of relatively low modulus and high water content perform significantly better as cell culture substrates, and that there is a “Goldilocks” zone that best promotes cell survival.^[7,8] One method that allows for tailoring of both modulus and water content of polymer coatings is the use of a layer-by-layer (LbL) approach to create polyelectrolyte multilayers (PEMs) from charged polyelectrolytes.^[9]

PEMs are films fabricated from polyelectrolytes (PEs), water-soluble polymers that contain a significant proportion of ionizable groups, and are assembled using an LbL method.^[10] PEs can either be polyanionic or polycationic, and their degree of ionization is controlled by pH. PEM deposition can be used to build up self-assembled polymer coatings onto substrates through electrostatic interactions by alternating polyanionic and polycationic polymers (Figure 1, top). Since being developed in the 1990s, PEMs have been used in areas such as macromolecular encapsulation,^[11] drug delivery,^[12] and biocompatible coatings for artificial implants.^[13] Much recent work has aimed to use PEMs as a “biocamouflage” coating between biological cells or tissues and engineered materials. Modulation of PEM fabrication conditions, such as deposition pH and choice of PEs, dramatically affects the resulting mechanical properties of the created PEM.^[14] Previous work has investigated cellular adhesion, proliferation, and differentiation of neural stem and progenitor cells, and subtypes of neural lineages (i.e., neurons, astrocytes, and oligodendrocytes) by tuning the Young’s modulus.^[15,16]

While PEMs have enjoyed a long history as coatings for biomedical applications,^[17] substantially less work has been conducted with neural cells from the central nervous system (CNS). Previous work attempted to use PEMs as a platform for neural cell proliferation and differentiation.^[18–20] Zhou et al. used an LbL assembled film of poly-ε-caprolactone, PLL, and heparin sulfates with the aim of increasing attachment, differentiation, and neurite outgrowth from neural progenitor cells.^[18,19] Ren and colleagues studied the contribution of surface effects from chemically distinct polymers on the differentiation and migration behavior of neural stem cells.^[21] Sailor et al. developed methodologies to create 2D poly(acrylic acid) (PAA) and poly(allylamine hydrochloride) (PAH) gradient films. These gradient films present the equivalent of over 10 000 single film experiments as one gradient surface and were used to determine the optimal assembly conditions for substrates that support the growth of HEK293 cells and embryonic rat spinal commissural neurons.^[7,8] Additionally, high content screening of cellular behavior using LbL-coated cell culture microplates has previously been studied for both C2C12 muscle cells and human periosteum-derived stem cells.^[22] These automatically generated films showed great promise as an additional methodology for easily creating large families of surfaces and demonstrated the facile versatility of LbL approaches for creating cell surfaces.

Here, we assessed PEM surfaces as substrates for neural cell growth, aiming to identify substrates that are more stable and

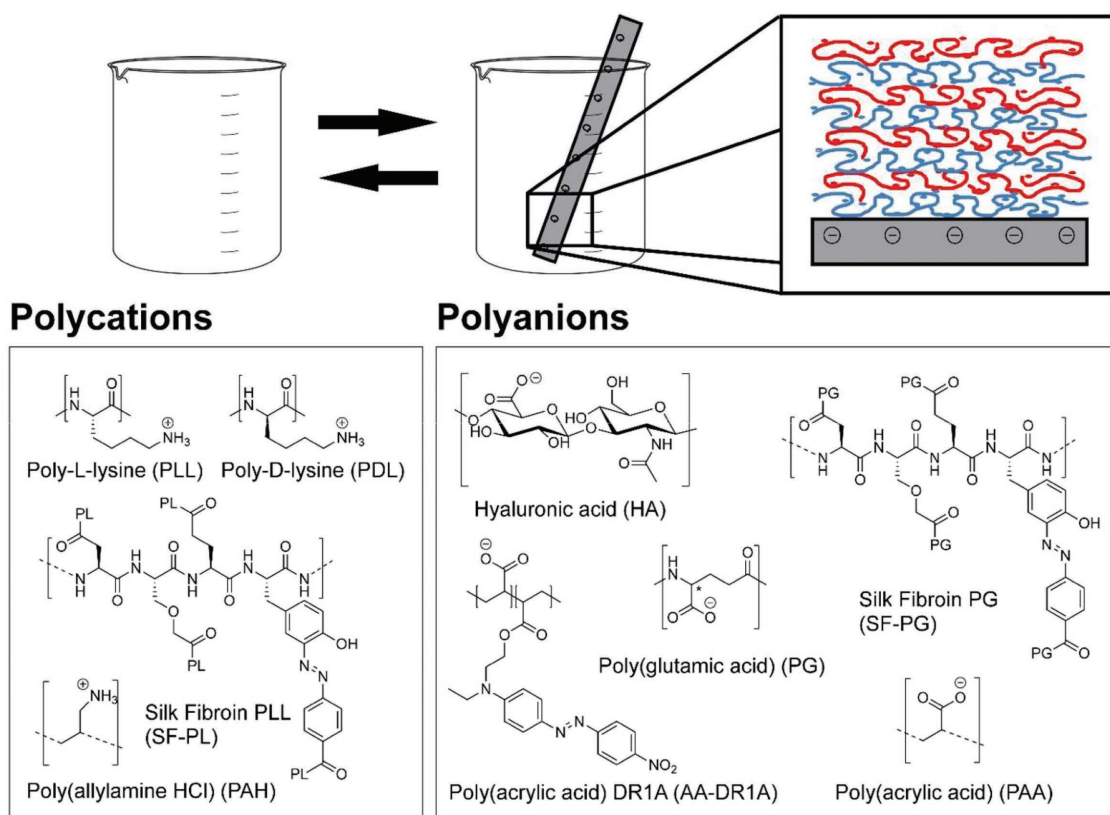


Figure 1. Top: Schematic depicting layer-by-layer assembly of PEM films, beginning with a negatively charged substrate (glass or silicon) being dipped in a polycation solution. Bottom: Illustration of biologically relevant polycationic and polyanionic polymers used in this study and their acronyms.

robust than PDL. We employed a set of guiding principles that aim to effectively “biocamouflage” less-than-optimal surfaces and create materials that are soft, wet, and “ECM-like” using an LbL approach. We evaluated the capacity of a catalog of PEMs to support neural growth and survival while rationalizing performance via the physicochemical properties of the different substrates. Our findings identified PEMs that exhibited enhanced neural biocompatibility to function as highly effective substrates to cultivate primary neural cells.

2. Results

2.1. Initial PEM Screening

To identify PEMs that best support neural cell attachment and survival, we started with the results of previous studies of gradient PAH/PAA systems and the best conditions identified from combinatorial pH assays of HEK293 cells and embryonic rat spinal commissural neurons.^[7,8] Due to the documented effectiveness of SF as an artificial ECM, we also included two new silk PEs: silk fibroin-co-poly-L-lysine (SF-PL) and silk fibroin-co-poly-L-glutamate (SF-PG). These specialized silk polymers were synthesized following published protocols with some modifications (see Section 5). All PEMs were assembled on plasma-cleaned coverslips (see Section 5) to a thickness of ten bilayers. Embryonic rat cortical neurons were cultured on each condition. Based on the gradient PAH/PAA films, the pH of deposition for PAH was chosen to be 5.5, and the pH of PAA was varied (5.0, 5.5, and 6.0). The deposition pH changes the charge density along each PE and alters the layer thickness by limiting attachment points to the surface (affecting how “loopy” each layer becomes). At the pKa of a PE, half of the possible ionizable groups on a PE are charged. For PAA, this pKa is at approximately pH = 5.5: pH values of deposition below 5.5 will make the polyanion less charged (longer loop length) and pH values above the pKa will make PAA more negatively charged (shorter loop length).^[8] The degree of charge along the backbone, and thus the loop length, influences modulus, thickness, and water content, which are key properties governing the capacity of these surfaces to support cell survival and growth.^[23] We varied the PAA deposition pH and examined the resultant capacity of the surfaces to support neuronal viability. For the silk polymers, the deposition pH was set to 7.4 based on previous investigation of PDL/PG multilayers.^[24] Neurons were cultured for 6 days before being fixed and stained with Alexa Fluor 488 Phalloidin to visualize F-actin and Hoechst 33258 to label nuclei. **Figure 2** illustrates neurons grown on each PEM compared to the control (PDL) and a blank coverslip. Based on qualitative assessment, films created using a PAA deposition pH of 5.0 exhibited poor growth and attachment, while higher cell density and networks of neurites were present for substrates assembled using a PAA deposition pH of 5.5 and 6.0 (Figure 2A–C).

To quantify the number of cells present, Hoechst 33258 stained nuclei were imaged and counted using Cell profiler software. This assay was used as a rapid screen for the capacity of a surface to promote cell attachment and survival. In the PAH/PAA pH study, cell survival and attachment decreased

on films constructed with a PAA deposition pH of 5.0. Films generated with PAA deposition pH values of 5.5 and 6.0 were not significantly different from each other or the control (Figure 2G). Compared to the PDL control, films constructed with pH values of 5.5 and pH 6.0 PAA deposition conditions were not significantly different in their capacity to support cell attachment and survival than PDL (ns, $p > 0.05$). From previous work, we discovered that films assembled with a deposition pH corresponding to that of the PE’s pKa supported maximum cellular survival and attachment. SF-PL/SF-PG performed similarly to the control condition (PDL, ns, $p > 0.05$). All conditions promoted cell attachment and survival better than an uncoated glass substrate ($p < 0.01$). This screen optimized the deposition pH and identified several materials that perform as well as PDL.

2.2. Optimizing Substrates to Promote Cell Survival and Growth

We altered the thickness and, as a result, the water content and modulus of each film by changing the deposition pH of each PE. Since each of the created films had the same number of layers, changes in thickness could be a pseudo-qualitative measurement of the water content of a film. As a method to characterize the substrates, the thickness of each film was measured by ellipsometry (Figure S1, Supporting Information). The best performing surface was generated using pH 5.5 for both PAH and PAA deposition, resulting in a 51 ± 1 nm thick film. The SF-PL/SF-PG film thickness was found to be 50 ± 6 nm, within the same range as the best PAH/PAA film. We detected a linear trend of increasing thickness with increasing pH for the PAH/PAA systems that correlated with increased cellular viability. A similar effect occurred using SF-PL/SF-PG, although it was not as pronounced as the trend in viability for PAH/PAA pH.

To better understand how the assembly conditions of PEM films influence neuronal survival and growth, we conducted a set of experiments that altered the number of bilayers. The performance of 2.5, 4.5, 8.5, and 12.5 bilayers were examined along with changing the deposition pH between the systems: PAH/PAA (pH = 4.5, 5.5, 6.5) and SF-PL/SF-PG (pH = 6.0, 7.0, 8.0). We chose to study the number of bilayers versus pH deposition, creating a pseudo-gradient of thickness for this screen. Cortical neurons were cultured on these surfaces, and the number of surviving cells counted and averaged over three cultures (Table S2 and Figure S2, Supporting Information). Counting the number of nuclei on each surface revealed a general trend; films created with 4.5 bilayers typically performed better than films created with 2.5 bilayers. Yet any number of bilayers above 4.5 showed no significant change in cell count. In general, a single monolayer of PDL (control) did not significantly differ from films with at least 4.5 bilayers (averaged).

Counting nuclei provides an easily automated measure of cell adherence and survival for each film. To assess the capacity of surfaces to promote process extension, we visualized the F-actin cytoskeleton by staining with fluorescent phalloidin. Interestingly, the surface with the most attached cells was not the same as the surface promoting the highest surface coverage (Figure 2H). SF-PL/SF-PG PEM (11.4% surface coverage) performed markedly better than both controls (PDL, 4.8%,

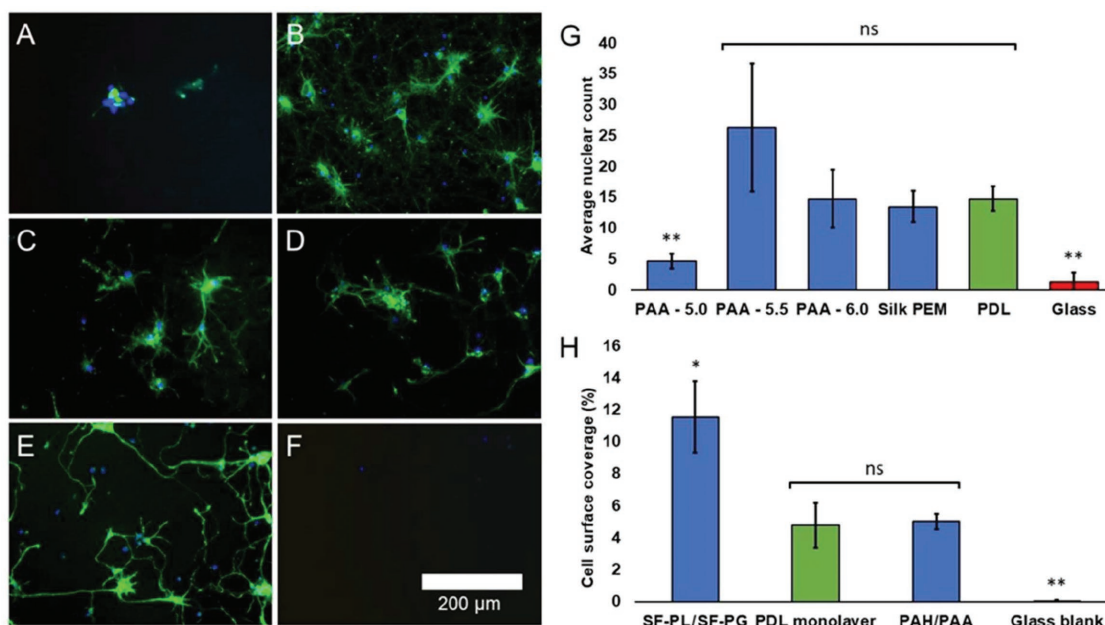


Figure 2. Assessing the survival (nuclei count) and growth (cell surface coverage) of the PAH/PAA and silk PEMs. Both materials perform competitively with PDL when quantifying nuclei count and cell surface coverage. All PEMs were 10 bilayers thick. A–F) Images of various PEM conditions. Each PEM film is terminated with a positive layer unless stated otherwise, and film thickness is denoted (in brackets). Cells were stained with Hoechst 33 258 (blue) to label nuclei and phalloidin Alexa Fluor 488 (green) to label F-actin. PEM conditions tested were: A) PAH/PAA with PAA at pH 5.0 (thickness = 23 nm), B) PAH/PAA with PAA at pH 5.5 (thickness = 51 nm), C) PAH/PAA with PAA at pH 6.0 (thickness = 99 nm), D) PDL-coated coverslip, E) SF-PL and SF-PG PEM (both at pH 7.0) (thickness = 39 nm), and F) blank coverslip. G) Quantifying cell surface coverage to compare PDL and silk-based and PAH/PAA-based PEMs. Compared to controls, SF-PL/SF-PG performed best and was significantly different than PDL and uncoated glass. PAH/PAA was better than bare glass but not significantly different than PDL. H) Surface area of phalloidin Alexa Fluor 488 staining to provide an estimate of cell size. ns ($p > 0.05$); * ($p \leq 0.05$); ** ($p \leq 0.01$); *** ($p \leq 0.001$).

$p < 0.05$, and glass, 0.04%, $p < 0.01$) and PAH/PAA (5.2%, $p > 0.05$) performed similar to PDL (control). While silk-based PEMs promoted cell attachment and viability similar to PDL, the capacity to support higher surface coverage was better than PAH/PAA surfaces. In contrast, PAH/PAA surfaces appear to be more adhesive, but are less effective at supporting cell spreading and process extension. A possible explanation is that PAH/PAA films may be substantially more adhesive than the SF films created, to the extent that they arrest neurite extension, while SF films are sufficiently adhesive to support cell survival, yet not to the extent that they inhibit cell and axon motility.

While the number of layers beyond 4.5 bilayers had no specific effect on viability, we can further test and tailor our surfaces by modifying PEM surface charge. So far, the terminal layer was always polycationic, but by adding an additional layer of polyanion, we can, in principle, change the surface to be negatively charged without significantly changing the thickness of the material. Previous research indicated that positively charged surfaces promote neuronal attachment^[25,26] and support the formation of high-density neural networks in culture. These studies utilized single monolayers of cationic PDL/PLL. In contrast, the multilayered materials we use here can partially mask the electrostatic charge of the outer layer that encounters the cellular plasma membrane. Typically, due to the plasma membrane phospholipid bilayer, cells exhibit a negative surface charge, perhaps accounting for positively charged polymers promoting cellular attachment.^[5,27] Within

a PEM, the charge of the outer surface layer may be partially masked by polymers extruded from the oppositely charged layer below, resulting in surface charge weakening with each subsequent layer.

To determine if neurons exhibit a preference for negative or positive outer layers on a PEM surface, we altered which layer was topmost for PAH/PAA and SF-PL/SF-PG PEMs. Neurons were then cultured on these surfaces for 12 days before fixation, stained, and quantified. Perhaps surprisingly, our findings indicate that the positive- and negative-terminated PEMs resulted in no significant difference in the number of nuclei present (Figure 3B). For the PEMs studied, the charge of the terminal layer did not appear to influence either the number of adherent cells (Figure 3B) or cell surface area (Figure 3A). It has been previously shown that negative charges within monolayered polymer materials perform poorly compared to polycationic polymers such as PLL/PDL^[26]; however, polyanionic polymers within multilayered materials support cellular attachment of neural cells.^[4,16] Interestingly, the absence of an effect of the charge of the outer layer extends to other PEM combinations, with cells generally showing little to no preference for positive- and negative-terminated PEMs (Figures S3 and S4, Supporting Information). The lack of top-layer charge preference may be due to the mixing of positive and negative polymer strands in thicker PEMs, or possibly due to binding of proteins from the cell culture medium or secreted by the cells that mask elements of the PEM terminal surface.

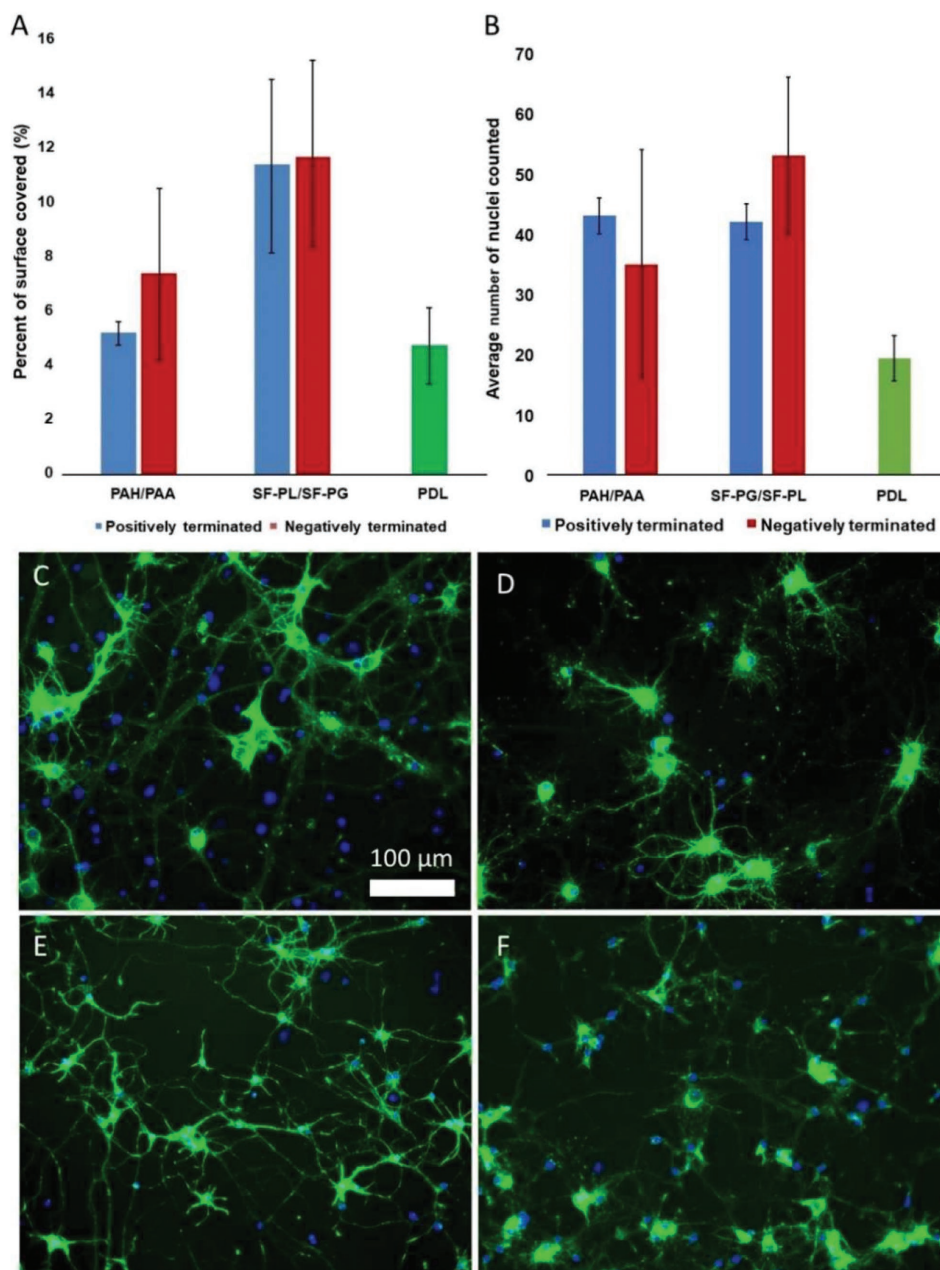


Figure 3. The charge of the terminal layer exhibits no significant effect on the growth and surface coverage of neural cells on PEM surfaces. A) No significant difference in cell surface coverage was found between positive- or negative-terminated PEMs composed of PAH/PAA or SF-PL/SF-PG. Comparison to PDL reveals that the silk-based PEMs perform significantly better for the positive- and negative-terminated surfaces ($p < 0.05$). B) No significant difference in the number of nuclei present was detected between positive- or negative-terminated PEMs composed of PAH/PAA or SF-PL/SF-PG. Compared to PDL, either silk-based PEM performed significantly better for both positive- and negative-terminated surfaces ($p < 0.05$). C–F) Representative images of each of the surfaces with the plated cortical neurons: C) PAH/PAA positively terminated, D) PAH/PAA negatively terminated, E) SF-PL/SF-PG positively terminated, and F) SF-PL/SF-PG negatively terminated.

2.3. Mechanical Characterization of PEMs

Modulus matching can enhance material biocompatibility for designer tissue engineering,^[18,28] and has been used to mask implants from rejection and aid in the generation of lab-derived tissues. The modulus of mammalian cortical brain tissue is on the order of 0.6–12 kPa, so employing exception-

ally soft polymers and coatings to more closely match this range of moduli has been proposed in order to reduce the rejection of neural implants.^[11,14] The importance of modulus within a material stems from an inverse relationship with water content. Higher water content materials tend to have lower modulus and high-modulus materials tend to have lower water content. To characterize the material generated

here, we performed nano-indentation on the SF-PL/SF-PG and PAH/PAA surfaces using an Asylum Research MFP-3D AFM to determine the modulus. Samples were freshly prepared in triplicate, and indented at nine different points, using a BL-TR400PB tip (Asylum Research, $k = 0.11 \text{ N m}^{-1}$) at an indentation rate of $5 \mu\text{m s}^{-1}$. An average of the indented values was calculated to obtain a value of $870 \pm 50 \text{ kPa}$, which is consistent with previous characterization of PAH/PAA surfaces,^[29] and the standard error is presented for each value. These values for SF-PL/SF-PG PEM were found to be substantially softer than PAH/PAA ($510 \pm 55 \text{ kPa}$). Comparing the Young's modulus of both materials indicated that the softer SF-PL/SF-PG PEM better supported cell spreading and process outgrowth compared to the stiffer PAH/PAA multilayer. These findings are in contrast with previous studies of endothelial cells which exhibit increased spreading on harder substrates.^[29] A meaningful comparison of the modulus of these multilayers to a single layer of PDL is essentially impossible, due to the difficulty of indenting a single layer of PDL on a glass substrate, where substrate effects overwhelm the measure and compromise obtaining an accurate indentation profile; however, a single molecular layer of PDL is expected to exhibit a similar high modulus as the underlying substrate.

2.4. Testing of Other Bio-Sourced PEMs

PEMs built from other natural polyelectrolytes such as hyaluronic acid (HA) and chitosan (CHI) were tested and found to support cell attachment and growth as well as, or better than, PDL. A wide range of PEs was explored to expand the testing set, including a host of naturally derived and bio-sourced polymers, assembled as we had standardized under the previously optimized parameters: 4.5 bilayers with positively terminated surfaces. All PEs used in this broader study are illustrated in Figure 1, including positively charged PLL and HA, and negatively charged poly(glutamic acid) (PG), poly(acrylic acid)-*co*-DR1A P(AA-*co*-DR1A), and CHI. A combinatorial approach was employed, testing all possible polyanion and polycation combinations in a 24-well cell culture plate (Figure S5, Supporting Information). Each multilayer was made by flooding the internal well with the PE of choice, waiting 5 min for electrostatic assembly to reach equilibrium, and then aspirating the excess away (full experimental details described in Section 5.). After washing twice with water, the alternate PE was added to the well, repeating the process until 4.5 bilayers were generated. Embryonic rat cortical neurons were then plated and cultured for 12 days. The cultures were then fixed, stained, and quantified (Tables S7 and S8, Supporting Information). PEMs containing HA as a polyanion performed significantly less well than PDL (control, $p < 0.001$), while polymers containing silk PEs, in general, performed significantly better than control. Neuronal viability appeared best when cultured on the SF-PL/P(AA-*co*-DR1A) PEM, which achieved a threefold increase in surface coverage as compared to PDL (control, $p < 0.001$). Notably, all PEMs that performed better than PDL contained a naturally derived PE (silk-based, PG, or PDL). The best performing

materials exhibited increased cell numbers and promoted higher surface coverage ($p < 0.05$). Figure 4 illustrates the PEMs in ascending order of surface coverage, assayed using F-actin labeled with fluorescent phalloidin, with the PDL control colored red.

Although a number of surfaces did not perform significantly different from PDL (control), three PEMs performed significantly better (Figure 4). PLL/P(AA-*co*-DR1A), SF-PL/SF-PG, and SF-PL/P(AA-*co*-DR1A) exhibited greatly enhanced cell growth when compared to PDL. Notably, all contain naturally derived polymers. The best among these was SF-PL/P(AA-*co*-DR1A) (15.5% surface coverage), which performed 3× better than PDL (5.5% surface coverage, control, $p < 0.001$) when comparing surface coverage. This trend was similar when counting the number of surviving cells (Figure S6, Supporting Information), with the exception of PLL/P(AA-*co*-DR1A) PEM, which dropped a few places in the ranking compared to the two top PEMs. While investigating the role of the polyanionic polymer, an interesting result was observed, that PAA and P(AA-DR1A) polyanions appeared to improve the survival and surface coverage of the cultured neurons. PAA and P(AA-DR1A) are both polymers based on poly(acrylic acid), while the P(AA-DR1A) polymer also contains a small functionalization fraction (1:19) of the azobenzene dye Disperse Red 1 (DR1). The azo dyes are often incorporated for other project goals, such as to visibly monitor the multilayers as they are building up on a surface and undergo testing to confirm stability, and also to permit external photo control to the polymer surface via the stimuli-responsive azo isomerization. Interestingly, the structures of the SF-PG and SF-PL polymers consist of a silk backbone with pendant co-polymers (either PG or PLL), in a “bottle brush” configuration, with silk as a backbone from which PG or PLL side-chains extend. However, each of the silk-based polymers performs markedly better than either PDL, or a film created from both PG and PL (control, $p < 0.05$). If performance was solely based on which surface was present, we would expect similar results from the silk-based polymers compared to the control or PLL/PG surfaces, which they do not. Notably, the best performing materials contained peptide linkages, which may contribute to these being particularly well tolerated by the neurons. The majority of the silk fibroin residues are neutral and not charged; thus, adding PDL or PG through typical peptide linkage chemistry is one way to augment the charge capability.

2.5. Identifying an Optimal Surface for Oligodendrocytes

By examining cortical neuron growth, we identified three multilayer systems that outperform a standard PDL monolayer and identified specific attributes of these systems that affect performance: thickness, chemical composition, and modulus. We then tested these systems using primary rat oligodendrocytes to determine if the enhanced substrate performance of the identified PEMs might generalize to this important vertebrate CNS glial cell type. Our findings indicated that oligodendrocytes exhibit some specificity for surface characteristics, but similar to the neurons, P(AA-*co*-DR1A)/SF-PL ranked highest in measures of extension and growth (Figure 5).

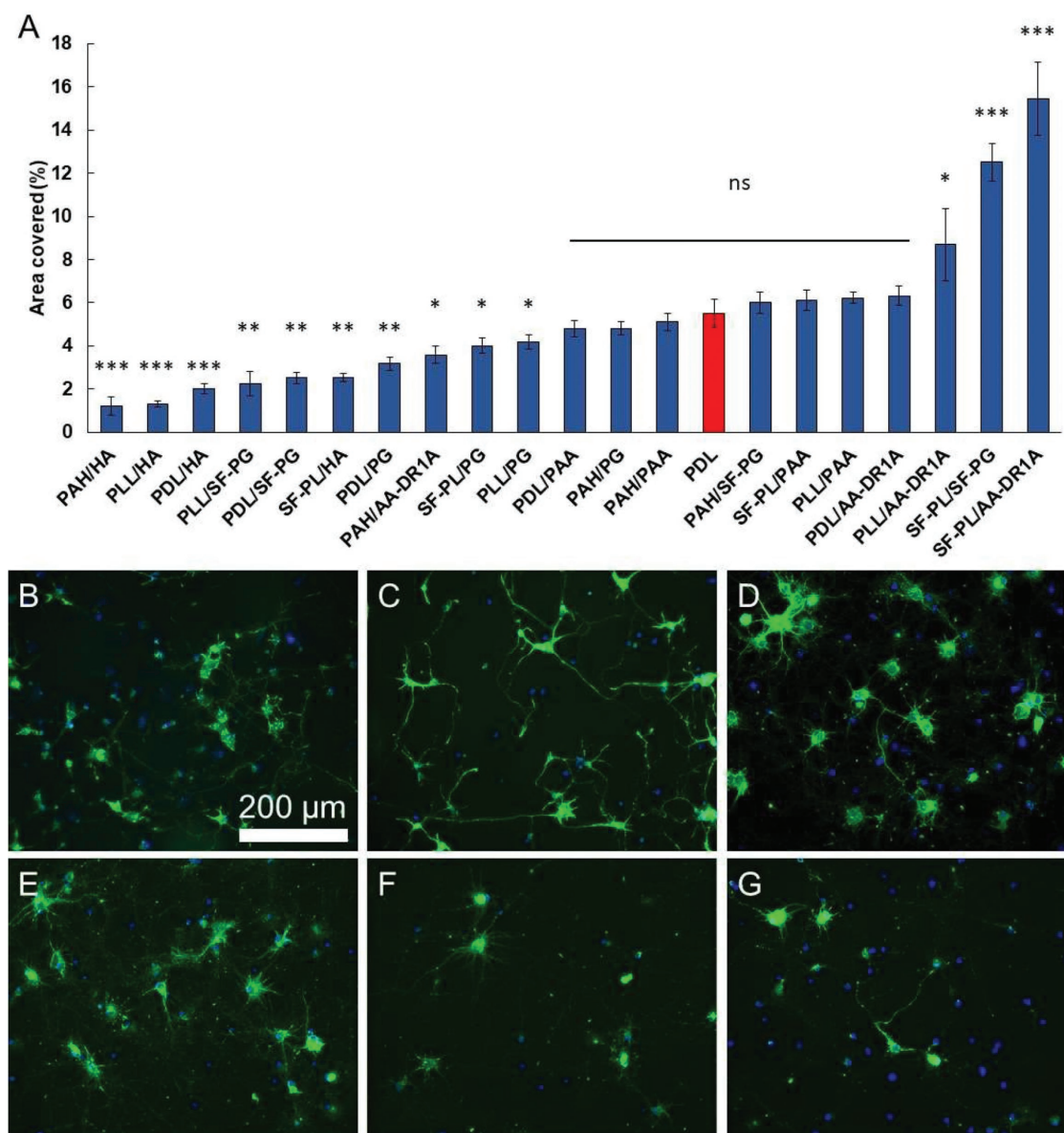


Figure 4. Combinatorial study of PEs ranking cell surface coverage. Thicknesses for all films are listed in Table S1, Supporting Information. A) Histogram showing PEMs ranked in ascending order of surface coverage. PDL control is red. All surfaces are 4.5 bilayers thick, positively charged, with deposition pH at the pKa of the polymer. B–G) Select images are shown for the following systems: B) PLL/SF-PG, C) SF-PL/P(AA-co-DR1A), D) SF-PG/SF-PL, E) PAA/PAH, F) HA/PLL, and G) control (PDL). ns ($p > 0.05$); * ($p \leq 0.05$); ** ($p \leq 0.01$); *** ($p \leq 0.001$).

Unlike the cortical neurons, this was the only PEM that scored significantly better than the PDL control ($p < 0.05$), while two other high-performing surfaces performed not significantly different from control (ns). HA-based PEMs again performed poorly, while PAH/PAA-based PEMs performed poorly as well. Silk-based PEs performed well, along with the majority of PEMs containing PDL or PLL. The capacity for these PEMs to be interchangeable while maintaining similar performance between vastly different neuronal cell types is a clear strength of this system. SF systems exhibited the best performance for both cell types, and specifically, the best and most optimized system SF-PL/P(AA-DR1A) was the top performer for both cell types.

3. Discussion

Systematic optimization of our PEM coatings using bio-inspired PEs has identified three coatings, each of which performs significantly better than PDL: SF-PL/SF-PG ($p \leq 0.001$), PLL/P(AA-DR1A) ($p < 0.05$), and SF-PL/P(AA-DR1A) ($p \leq 0.001$). While the synthetic PEM (PAH/PAA) performed similarly to PDL when measuring cellular attachment, ultimately silk-based PEMs proved to be significantly better than PDL or synthetic PEs when measuring surface coverage. These results were the culmination of several iterations of development, which required the optimization of the number of layers, the pH of

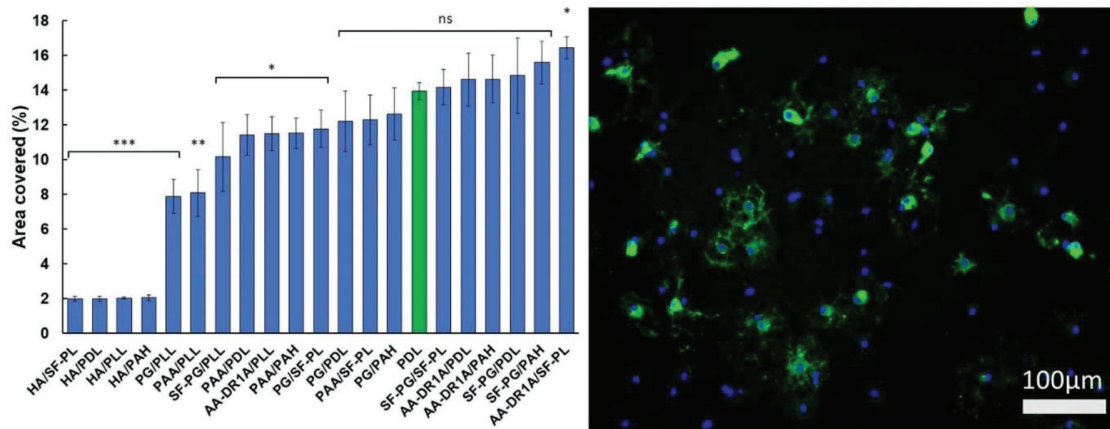


Figure 5. Oligodendrocytes cultivated on P(AA-DR1A)/SF-PL films exhibit significantly better area coverage compared to PDL ($p < 0.05$). Combinatorial study ranking cell surface coverage for each PEM for rodent oligodendrocytes. Thicknesses for all films are listed in Table S1, Supporting Information. Left: Histogram shows PEMs ranked in ascending order of surface coverage. PDL control is green. All surfaces are 4.5 bilayers thick, positively charged, and the deposition pH is the pKa of the polymer. Right: Representative micrograph of the P(AA-DR1A)/SF-PL PEM showing F-actin labeling (green) and nuclear stain (blue). ns ($p > 0.05$); * ($p \leq 0.05$); ** ($p \leq 0.01$); *** ($p \leq 0.001$).

deposition, and modification of terminal charge. The assembly of PEMs onto a non-compatible surface functions as biocamouflage, making the new coated surface relatively more soft and wet, with a composition that resembles an ECM. All of these properties contribute to creating an effective and functional synthetic ECM substrate for neural cells.

The Young's modulus, chemical functionality, and water content all play major roles in successful biocamouflage, and we varied each of these properties within our study with the aim of creating superior substrate coatings for neural cell culture. Low modulus materials have been previously shown to affect the motility and physical spreading of cells.^[30,31] Further, relatively low modulus gels have shown promise to prevent astrocyte spreading and to reduce astrocyte recruitment during gliosis, effectively delaying the formation of a glial scar.^[32] We found that the SF-PG/SF-PL PEM has an indentation modulus that is significantly softer than PAH/PAA at 510 ± 55 kPa. This value for the optimal silk surfaces corresponds well with an optimal range of 500–800 kPa previously identified for cultured embryonic rat spinal commissural interneurons.^[7] Intriguingly, the high-functioning PAA/PAH surfaces possess a modulus of 870 ± 50 kPa, which is slightly outside the previously identified ideal range, suggesting that it may be possible to further optimize these surfaces. Striking the appropriate balance between being not too soft or too stiff is important, as modulus can prevent cells from adhering or from extending processes and thereby limit neural network formation.^[30,33]

Chemically similar polymer coatings have been found to trigger dramatically different cellular responses, and thus, polymer selection can dramatically affect the success of neural regeneration or cultivation.^[32,34] Since a wide range of responses can be found, we used a combinatorial approach for screening the viability of each PEM coating. We found that in general, HA-based PEMs performed significantly less well than PDL and were the lowest performing materials. This was surprising since HA is a major structural component within the CNS; however, it may function more as a structural scaffold for other macromolecules in vivo, rather than directly interacting

with cells to promote adhesion and process extension.^[35] A striking finding we obtained is that any PE which contained a peptide backbone performed as well or better than PDL. Our combinatorial search highlighted silk-based PEMs, suggesting that these are promising materials for coatings. Silk has been previously explored as a functional material for numerous applications including regenerative medicine,^[36,37] functioning as an artificial extracellular matrix, specifically designed to promote the growth of neural tissues. Notably, Gu and colleagues have employed the lower modulus of *Bombyx mori* silk in conjunction with cellulose and relatively high tensile strength of spider silk to create nerve grafts.^[36] Cellulose and spider silk provide a rope-like physical guidance scaffold, while *B. mori* silk provides an optimal growth medium with low modulus.

Poly-lysine has remained a standard material for coating substrates for several decades; however, PDL and PLL both are relatively expensive to produce and are prone to degradation and thus the coated substrates need to be made immediately prior to use. The PEM coating materials we describe here are based on silk fibroin, a relatively inexpensive natural polymer source. When assembled into a PEM, a relatively simple coating of SF-PL/SF-PG performs significantly better than PDL. These materials can be assembled weeks prior to plating and are relatively shelf stable as compared to less robust PL coatings. Silk fibroin is a polypeptide and, therefore, is prone to proteolytic degradation, yet when assembled into a thick PEM coating, it can last for several months.^[38] Further, PEM formation is not limited to substrates, but have the capacity to coat irregular surfaces. Silk-based PEMs may also have substantial potential as coatings to promote the neural biocompatibility of biomedical devices implanted in the CNS in vivo.

4. Conclusions

By optimizing the choice of various PE employed, the pH of deposition, and the number of layers, we identified new sets of

PE combinations to create a PEM that performs significantly better as a substrate for neural cell growth than standard PDL. These experimental results were measured on two matrices of quantification: a survival assay (number of nuclei present) and a growth assay (surface area of cell coverage). PEMs created with SF-PL (a polymer containing silk fibroin from *B. mori* silk worms co-polymerized with PLL) and P(AA-co-DR1A) or SF-PG substantially outperformed PDL. The silk polymers themselves contain PG and PLL (depending on PE) as a co-polymer, yet perform better than either PDL or PG on all matrices measured. We demonstrate that employing silk results in a softer modulus for the assembled PEM (510 ± 55 kPa versus 870 ± 50 kPa). These newly developed materials have potential applications as improved supports for neural cell culture in vitro and also as coatings for devices and implants to enhance neural biocompatibility in vivo.

5. Experimental Section

Materials and Methods: All polymers, reagents, and salts used in the fabrication of PEM films were purchased from Sigma-Aldrich. Silk fibroin with appended polyglutamate (SF-PG) and silk fibroin with appended poly-L-lysine (SF-PL) were synthesized as described,^[23] with some modifications. Silk fibroin for these procedures was provided by Tajima Shoji Ltd. (Yokohama, Japan). Poly((acrylic acid)-co-DR1A) (19:1) P(AA-co-DR1A) was prepared as described.^[39] The 24-well glass bottom plates were purchased from Greiner Bio-One (Monroe, USA). Distilled water was purified by a Milli-Q purification system (Millipore, Billerica, USA) for the preparation of all solutions. The pH of all solutions was measured using a SympHony B10P pH meter with an immersion probe and a KI electrolyte solution (VWR, Radnor, USA). Film thickness was measured using an M-033K001 Optrel Multiskop ellipsometer (Sinzing, DE). Glass coverslip substrates were cleaned using a plasma cleaner (Harrick Plasma, Ithaca, USA) prior to PEM deposition. Images were acquired using an Axiovert 100 inverted fluorescence microscope (Carl Zeiss Canada, Toronto, Canada) with a MagnaFire CCD camera and MagnaFire 4.1C imaging software (Optronics, Goleta, USA). Images were further processed using ImageJ 2.0 (Open-Source, Madison, USA) and CellProfiler Version 2.0 (Open-Source, Cambridge, USA) for cell counting.

Silk Fibroin-co-poly-L-glutamate and Silk Fibroin-co-poly-L-lysine Synthesis: Methods for the preparation of silk solutions from *B. mori* silkworm cocoons were based on protocols from Rockwood et al.^[40] Both SF-PG and SF-PL were synthesized as previously described with some modifications.^[24] To a vial equipped with a stir bar, 1.25 mL of a 0.2 M 4-aminobenzoic acid solution (in acetonitrile) was added along with 625 μ L of a 1.6 M *p*-toluene sulfonic acid aqueous solution. The resulting solution was cooled to 5 °C in an ice bath. A 0.2 M NaNO₂ aqueous solution, 625 μ L, was added to the cooled flask dropwise which produced a bright yellow diazonium salt solution. The solution was stirred for 25 min on ice. Two milliliters of a 5% w/v silk solution and 0.25 mL of a 1 M boric acid/sodium borate buffer solution was added to a separate vial, mixed, and cooled to 5 °C. The silk solution was adjusted to pH 9 and 0.5 mL of the diazonium salt solution was added dropwise over 2 min. This addition produced a bright red solution that was stirred for 30 min on ice. The red azobenzene-modified silk solution was purified using desalinating columns (NAP-25, VWR International) with distilled water as the eluent. Once the azobenzene-modified silk solution was purified, enough chloroacetic acid was added to produce a 1.0 M solution (roughly 1.2 mL). Immediately after the addition, a white precipitate formed, that slowly dissolved back into solution with additional stirring. The solution was stirred for 1 h at room temperature and produced a hazy orange colored solution. The resulting solution was loaded into a Slide-A-Lyzer dialysis cassette (3500 MW, 3–12 mL) and was dialyzed against water for 72 h (the water was changed thrice).

The resulting solution was divided into two batches, one for producing SF-PL and one for producing SF-PG. Roughly 3 mL of the mother solution was added to each 8 dram vial and stirred. PDL, 0.502 g, was added to one vial and PG, 0.532 g, was added to the other. The pH of the resulting solutions was adjusted to 6 using dilute HCl and 60 mg of EDC (1-ethyl-3-(3-dimethylaminopropyl)carbodiimide) added to both vials and stirred at rt for 8 h. After the reaction was completed, the resulting polymer solution was dialyzed against water for 72 h and the water was changed twice. The solution was diluted to 0.5 mg mL⁻¹ for use in PEM fabrication. NMR spectra of the final products were taken by adding 10% deuterated water and adding deuterated benzene. NMR signals observed corresponded to literature values.^[24] SF-PL: ¹H NMR (300 MHz, 10% D₂O, Benzene-*d*₆ insert): δ 0.71 (br, Val), 1.25–1.31 (m, Lys), 1.55 (m, Lys/Lys), 2.84 (m, br, Lys), 3.55 (s, –CH₂–COO), 3.73 (m, Ser/Gly), 4.15 (m, Lys), 6.81–7.05 (m, trace, Tyr + Azo). SF-PG: ¹H NMR (300 MHz, 10% D₂O, Benzene-*d*₆ insert): δ 0.71 (br, Val), 1.21 (br, Ala), 1.52–2.05 (m, Glu), 2.13 (m, Glu), 3.55 (s, –CH₂–COO), 3.78 (m, Ser/Gly), 4.16 (m, Glu), 6.81–7.07 (m, trace, Tyr + Azo).

PEM Fabrication: Polyelectrolyte solutions were prepared at a concentration of 0.5 mg mL⁻¹ using Milli-Q deionized water. The pH of the deposition solution was adjusted to the desired value using 1 M NaOH or 1 M HCl solutions. Each surface was cleaned with a plasma cleaner prior to use. One milliliter of the positive PE solution was placed onto the surface of choice and allowed to self-assemble into a layer for 10 min. The positive PE solution was then removed with a pipette, and the surface was washed thrice (3 \times 1 mL) with deionized water. Filtered air was used to dry the surface prior to the deposition of the negative PE solution onto the surface for 10 min. The negative PE solution was then removed with a pipette and the surface washed in the same manner as with the positive PE solution. This procedure was repeated until the desired number of layers was built up.

Ellipsometry Measurements: The thickness of fabricated PEM surfaces was measured using a single wavelength (633 nm, non-absorbing) null-ellipsometer (Optrel Multiskop, Germany) using a fixed angle of 70° (140° between source and detector). Measurements were performed on dried samples, using a model that had two layers on silicon ($n = 3.42$, $k = -0.011$): silicon dioxide ($t = 2.3$ nm, $n = 1.54$) and an unknown polymer layer ($t = x$, $n = y$), under air ($n = 1.00$). The model was fit assuming the refractive index of the PEM was the average of the two polymers separately and was used as a starting point for data fitting. Table S1, Supporting Information, shows the combinations of averaged film thicknesses, and each noted thickness was calculated from a series of three measurements from three prepared samples.

Neural Cell Culture: Oligodendroglial and cortical neuronal cell cultures were derived from Sprague-Dawley rats (Charles River, Senneville, Canada). All procedures were performed in accordance with the Canadian Council on Animal Care guidelines for the use of animals in research and approved by the Montreal Neurological Institute Animal Care Committee and the McGill Animal Compliance Office. Embryonic rat cortical neurons were obtained by dissection of embryonic day 16–17 (E16/17) Sprague-Dawley rat brain (Charles River, Senneville, Canada) as previously described.^[41] Prepared 24-well plates were irradiated for 20 min to ensure sterility of the surfaces. Neurons were plated at a density of 50 000 cells per well. Cultures were maintained for 14 days in Neurobasal medium containing 1% B27 (Life Technologies, Carlsbad, USA), 1% penicillin/streptomycin (Life Technologies), 0.5% N-2 supplement (Life Technologies), 0.25% GLUTAMax (Life Technologies), and 0.2% Fungizone antimycotic (Life Technologies) in a 37 °C incubator with 5% carbon dioxide (Thermo Fisher Scientific).

Oligodendrocyte precursor cells were obtained from mixed glial cultures derived from postnatal day 0 (P0) rat pups and grown in oligodendrocyte defined medium as described with 0.1% fetal bovine serum included to initiate differentiation.^[42] Oligodendrocytes were plated at a density of 40 000 cells per well. Cells were fixed by immersion in a 4% solution of paraformaldehyde (PFA) (Thermo Fisher Scientific, Waltham, USA) in phosphate buffered saline (PBS) for 20 min. PFA was removed, and the surfaces washed twice for 10 min with PBS. Blocking was then performed for 1 h using a solution of 0.25% Triton X-100 (Thermo Fisher Scientific)



and 3% horse serum (HS) (Life Technologies) in PBS. Secondary antibody was prepared using Alexa Fluor Phalloidin 488 (Life Technologies) at a concentration of 1:1000 and Hoechst 33258 (Life Technologies) at a concentration of 1:3000 in PBS with 1% HS. The secondary antibody was incubated for 2 h, and surfaces washed thrice for 10 min with PBS. Surfaces were then immersed in PBS in preparation for imaging.

Image Processing: Cells were imaged using an Axiovert 100 inverted fluorescence microscope (Carl Zeiss Canada, Toronto, Canada) with a Magnafire CCD camera and MagnaFire 4.1C imaging software (Optronics, Goleta, USA). To assess the effectiveness of each multilayer system, cells were stained with Hoechst 33258 (nuclear stain) and with Alexa Fluor Phalloidin 488 labeling of F-actin and quantified using Cell Profiler (Broad Institute, Cambridge, USA) and Fiji version 1.0.^[43] A series of six micrographs were taken from each well independently, blind to the experimental conditions. Two characteristics of each image were then assessed: the average number of adherent cells (Hoechst 33258) and total surface area of the cell body including processes (Alexa Fluor Phalloidin 488). Both values were calculated using the Cell Profiler application. To standardize, the number of nuclei and surface area were tabulated from each image and averages calculated per condition, and this average was calculated for each surface condition and compared against a control of PDL. Each condition was replicated thrice to ensure reproducibility. Statistical analyses, including analysis of variance (ANOVA, least significant difference), were performed using SPSS 21 (IBM, Armonk, USA).

Supporting Information

Supporting Information is available from the Wiley Online Library or from the author.

Acknowledgements

The authors are grateful to Dr. Beatrice Lego and Mohini Ramkaran for their assistance with the AFM indentation measurements. The project was supported by a Collaborative Health Research Program (CHRP) grant from the Canadian Institutes of Health Research (CIHR 357055) and the Natural Sciences and Engineering Research Council (NSERC 493633-16). T.C.C., M.J.L., T.E.K., and C.J.B. are grateful to the NSERC CREATE program (Canada) for supporting interdisciplinary collaboration through the McGill/MNI Training Grant in NeuroEngineering. Support for the project (MSSoC#3009) and a studentship to D.S.N. was provided by the Multiple Sclerosis Society of Canada.

Conflict of Interest

The authors declare no conflict of interest.

Keywords

bio-camouflage, extracellular matrix, neural cells, polyelectrolyte multilayers, silk

Received: February 7, 2019

Revised: March 12, 2019

Published online: April 2, 2019

- [1] a) M. J. Landry, F.-G. Rollet, T. E. Kennedy, C. J. Barrett, *Langmuir* **2018**, *34*, 8709; b) J. M. Aamodt, D. W. Grainger, *Biomaterials* **2016**, *86*, 68; c) R. Bellamkonda, J. P. Ranieri, N. Bouche, P. Aebischer,

- J. Biomed. Mater. Res.* **1995**, *29*, 663; d) E. S. Gil, S. H. Park, J. Marchant, F. Omenetto, D. L. Kaplan, *Macromol. Biosci.* **2010**, *10*, 664.
- [2] D. Yates, *Nat. Rev. Neurosci.* **2012**, *13*, 288.
- [3] Z. Yavin, E. Yavin, *Dev. Biol.* **1980**, *75*, 454.
- [4] P. Roach, T. Parker, N. Gadegaard, M. R. Alexander, *Surf. Sci. Rep.* **2010**, *65*, 145.
- [5] Y. H. Kim, N. S. Baek, Y. H. Han, M. A. Chung, S. D. Jung, *J. Neurosci. Methods* **2011**, *202*, 38.
- [6] L. J. Millet, M. U. Gillette, *Yale. J. Biol. Med.* **2012**, *85*, 501.
- [7] M. Sailer, K. L. W. Sun, O. Mermut, T. E. Kennedy, C. J. Barrett, *Biomaterials* **2012**, *33*, 5841.
- [8] M. Sailer, C. J. Barrett, *Macromolecules* **2012**, *45*, 5704.
- [9] A. J. Karlsson, R. M. Flessner, S. H. Gellman, D. M. Lynn, S. P. Palecek, *Biomacromolecules* **2010**, *11*, 2321.
- [10] a) G. Decher, *Science* **1997**, *277*, 1232; b) G. Decher, J. D. Hong, J. Schmitt, *Thin Solid Films* **1992**, *210-211*, 831.
- [11] a) I. L. Radtchenko, G. B. Sukhorukov, S. Leporatti, G. B. Khomutov, E. Donath, H. Mohwald, *J. Colloid Interface Sci.* **2000**, *230*, 272; b) G. B. Sukhorukov, A. A. Antipov, A. Voigt, E. Donath, H. Mohwald, *Macromol. Rapid Commun.* **2001**, *22*, 44; c) D. V. Volodkin, A. I. Petrov, M. Prevot, G. B. Sukhorukov, *Langmuir* **2004**, *20*, 3398; d) H. Zhu, M. J. McShane, *Langmuir* **2005**, *21*, 424.
- [12] a) J. Almodovar, S. Bacon, J. Gogolski, J. D. Kisiday, M. J. Kipper, *Biomacromolecules* **2010**, *11*, 2629; b) S. De Koker, R. Hoogenboom, B. G. De Geest, *Chem. Soc. Rev.* **2012**, *41*, 2867.
- [13] a) J. Jagur-Grodzinski, *Polym. Adv. Technol.* **2006**, *17*, 395; b) P. Schultz, D. Vautier, L. Richert, N. Jessel, Y. Haikel, P. Schaaf, J. C. Voegel, J. Ogier, C. Debry, *Biomaterials* **2005**, *26*, 2621.
- [14] M. T. Thompson, M. C. Berg, I. S. Tobias, M. F. Rubner, K. J. Van Vliet, *Biomaterials* **2005**, *26*, 6836.
- [15] V. Gribova, R. Auzely-Velty, C. Picart, *Chem. Mater.* **2012**, *24*, 854.
- [16] S. Kidambi, I. Lee, C. Chan, *Adv. Funct. Mater.* **2008**, *18*, 294.
- [17] T. Boudou, T. Crouzier, K. Ren, G. Blin, C. Picart, *Adv. Mater.* **2010**, *22*, 441.
- [18] K. Zhou, G. Z. Sun, C. C. Bernard, G. A. Thouas, D. R. Nisbet, J. S. Forsythe, *Biointerphases* **2011**, *6*, 189.
- [19] K. Zhou, G. A. Thouas, C. C. Bernard, D. R. Nisbet, D. I. Finkelstein, D. Li, J. S. Forsythe, *ACS Appl. Mater. Interfaces* **2012**, *4*, 4524.
- [20] K. Ren, T. Crouzier, C. Roy, C. Picart, *Adv. Funct. Mater.* **2008**, *18*, 1378.
- [21] a) Y. J. Ren, H. Zhang, H. Huang, X. M. Wang, Z. Y. Zhou, F. Z. Cui, Y. H. An, *Biomaterials* **2009**, *30*, 1036; b) Y. J. Ren, Z. Y. Zhou, B. F. Liu, Q. Y. Xu, F. Z. Cui, *Int. J. Biol. Macromol.* **2009**, *44*, 372.
- [22] P. Machillot, C. Quintal, F. Dalonneau, L. Hermant, P. Monnot, K. Matthews, V. Fitzpatrick, J. Liu, I. Pignot-Paintrand, C. Picart, *Adv. Mater.* **2018**, *30*, 1801097.
- [23] a) A. J. Engler, L. Richert, J. Y. Wong, C. Picart, D. E. Discher, *Surf. Sci.* **2004**, *570*, 142; b) M. Ozzy, L. Julie, G. G. Derek, C. J. Barrett, *Macromolecules* **2003**, *36*, 8819.
- [24] M. A. Serban, D. L. Kaplan, *Biomacromolecules* **2010**, *11*, 3406.
- [25] R. F. Valentini, T. G. Vargo, J. A. Gardella, P. Aebischer, *J. Biomater. Sci., Polym. Ed.* **1994**, *5*, 13.
- [26] K. Webb, V. Hlady, P. A. Tresco, *J. Biomed. Mater. Res.* **1998**, *41*, 422.
- [27] a) P. C. Letourneau, *Dev. Biol.* **1975**, *44*, 77; b) E. Yavin, Z. Yavin, *J. Cell Biol.* **1974**, *62*, 540.
- [28] O. Etienne, A. Schneider, J. A. Kluge, C. Bellemin-Lapponaz, C. Polidori, G. G. Leisk, D. L. Kaplan, J. A. Garlick, C. Egles, *J. Periodontol.* **2009**, *80*, 1852.
- [29] A. Schneider, G. Francius, R. Obeid, P. Schwinté, J. Hemmerlé, B. Frisch, P. Schaaf, J.-C. Voegel, B. Senger, C. Picart, *Langmuir* **2006**, *22*, 1193.
- [30] a) S. Bai, W. Zhang, Q. Lu, Q. Ma, D. L. Kaplan, H. Zhu, *J. Mater. Chem. B* **2014**, *2*, 6590; b) A. Banerjee, M. Arha, S. Choudhary,

- R. S. Ashton, S. R. Bhatia, D. V. Schaffer, R. S. Kane, *Biomaterials* **2009**, *30*, 4695.
- [31] a) M. Cheng, J. Deng, F. Yang, Y. Gong, N. Zhao, X. Zhang, *Biomaterials* **2003**, *24*, 2871; b) N. D. Leipzig, M. S. Shoichet, *Biomaterials* **2009**, *30*, 6867.
- [32] M. T. Fitch, J. Silver, *Exp. Neurol.* **2008**, *209*, 294.
- [33] T. T. Yu, M. S. Shoichet, *Biomaterials* **2005**, *26*, 1507.
- [34] W. Huang, R. Begum, T. Barber, V. Ibba, N. C. Tee, M. Hussain, M. Arastoo, Q. Yang, L. G. Robson, S. Lesage, T. Gheysens, N. J. Skaer, D. P. Knight, J. V. Priestley, *Biomaterials* **2012**, *33*, 59.
- [35] X. Wang, J. He, Y. Wang, F.-Z. Cui, *Interface Focus* **2012**, *2*, 278.
- [36] a) C. Y. Wang, K. H. Zhang, C. Y. Fan, X. M. Mo, H. J. Ruan, F. F. Li, *Acta Biomater.* **2011**, *7*, 634; b) Y. Wei, K. Gong, Z. Zheng, A. Wang, Q. Ao, Y. Gong, X. Zhang, *J. Mater. Sci.: Mater. Med.* **2011**, *22*, 1947.
- [37] Y. Wang, D. D. Rudym, A. Walsh, L. Abrahamsen, H. J. Kim, H. S. Kim, C. Kirker-Head, D. L. Kaplan, *Biomaterials* **2008**, *29*, 3415.
- [38] T. Arai, G. Freddi, R. Innocenti, M. Tsukada, *J. Appl. Polym. Sci.* **2004**, *91*, 2383.
- [39] N. M. Ahmad, M. Saqib, C. J. Barrett, *J. Macromol. Sci. A* **2010**, *47*, 571.
- [40] D. N. Rockwood, R. C. Preda, T. Yucel, X. Wang, M. L. Lovett, D. L. Kaplan, *Nat. Protoc.* **2011**, *6*, 1612.
- [41] J. S. Goldman, M. A. Ashour, M. H. Magdesian, N. X. Tritsch, S. N. Harris, N. Christofi, R. Chemali, Y. E. Stern, G. Thompson-Steckel, P. Gris, S. D. Glasgow, P. Grutter, J. F. Bouchard, E. S. Ruthazer, D. Stellwagen, T. E. Kennedy, *J. Neurosci.* **2013**, *33*, 17278.
- [42] a) R. C. Armstrong, *Methods* **1998**, *16*, 282; b) A. A. Jarjour, C. Manitt, S. W. Moore, K. M. Thompson, S.-J. Yuh, T. E. Kennedy, *J. Neurosci.* **2003**, *23*, 3735.
- [43] J. Schindelin, I. Arganda-Carreras, E. Frise, V. Kaynig, M. Longair, T. Pietzsch, S. Preibisch, C. Rueden, S. Saalfeld, B. Schmid, J.-Y. Tinevez, D. J. White, V. Hartenstein, K. Eliceiri, P. Tomancak, A. Cardona, *Nat. Methods* **2012**, *9*, 676.